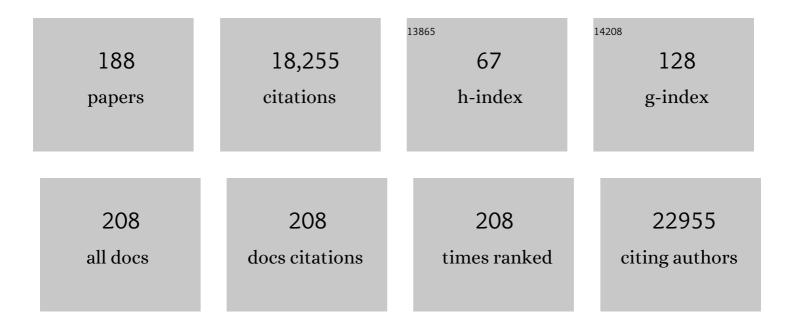
Karl-Peter Hopfner

List of Publications by Year in descending order

Source: https://exaly.com/author-pdf/4563729/publications.pdf Version: 2024-02-01



#	Article	IF	CITATIONS
1	cGAS produces a 2′-5′-linked cyclic dinucleotide second messenger that activates STING. Nature, 2013, 498, 380-384.	27.8	1,193
2	Structural Biology of Rad50 ATPase. Cell, 2000, 101, 789-800.	28.9	886
3	Molecular mechanisms and cellular functions of cGAS–STING signalling. Nature Reviews Molecular Cell Biology, 2020, 21, 501-521.	37.0	846
4	Structural mechanism of cytosolic DNA sensing by cGAS. Nature, 2013, 498, 332-337.	27.8	608
5	Modulation of protein properties in living cells using nanobodies. Nature Structural and Molecular Biology, 2010, 17, 133-138.	8.2	494
6	The Rad50 zinc-hook is a structure joining Mre11 complexes in DNA recombination and repair. Nature, 2002, 418, 562-566.	27.8	485
7	The C-Terminal Regulatory Domain Is the RNA 5′-Triphosphate Sensor of RIG-I. Molecular Cell, 2008, 29, 169-179.	9.7	458
8	Structural Biochemistry and Interaction Architecture of the DNA Double-Strand Break Repair Mre11 Nuclease and Rad50-ATPase. Cell, 2001, 105, 473-485.	28.9	448
9	Structural Biochemistry of a Bacterial Checkpoint Protein Reveals Diadenylate Cyclase Activity Regulated by DNA Recombination Intermediates. Molecular Cell, 2008, 30, 167-178.	9.7	366
10	5′-triphosphate RNA requires base-paired structures to activate antiviral signaling via RIG-I. Proceedings of the National Academy of Sciences of the United States of America, 2009, 106, 12067-12072.	7.1	348
11	cGAS senses long and HMGB/TFAM-bound U-turn DNA by forming protein–DNA ladders. Nature, 2017, 549, 394-398.	27.8	346
12	Cytosolic Viral Sensor RIC-I Is a 5'-Triphosphate–Dependent Translocase on Double-Stranded RNA. Science, 2009, 323, 1070-1074.	12.6	325
13	Crosstalk between the cGAS DNA Sensor and Beclin-1 Autophagy Protein Shapes Innate Antimicrobial Immune Responses. Cell Host and Microbe, 2014, 15, 228-238.	11.0	291
14	Structural basis for DNA duplex separation by a superfamily-2 helicase. Nature Structural and Molecular Biology, 2007, 14, 647-652.	8.2	281
15	Epitope interactions of monoclonal antibodies targeting CD20 and their relationship to functional properties. MAbs, 2013, 5, 22-33.	5.2	280
16	Establishment of Sister Chromatid Cohesion at the S. cerevisiae Replication Fork. Molecular Cell, 2006, 23, 787-799.	9.7	268
17	Cytosolic RNA:DNA hybrids activate the <scp>cGAS</scp> –STING axis. EMBO Journal, 2014, 33, 2937-2946.	7.8	257
18	Mutations affecting the secretory COPII coat component SEC23B cause congenital dyserythropoietic anemia type II. Nature Genetics, 2009, 41, 936-940.	21.4	250

#	Article	IF	CITATIONS
19	Syk Kinase-Coupled C-type Lectin Receptors Engage Protein Kinase C-δ to Elicit Card9 Adaptor-Mediated Innate Immunity. Immunity, 2012, 36, 32-42.	14.3	249
20	OAS proteins and cGAS: unifying concepts in sensing and responding to cytosolic nucleic acids. Nature Reviews Immunology, 2014, 14, 521-528.	22.7	246
21	X-Ray Structures of the Sulfolobus solfataricus SWI2/SNF2 ATPase Core and Its Complex with DNA. Cell, 2005, 121, 363-373.	28.9	228
22	Roles of RIG-I N-terminal tandem CARD and splice variant in TRIM25-mediated antiviral signal transduction. Proceedings of the National Academy of Sciences of the United States of America, 2008, 105, 16743-16748.	7.1	219
23	Structural basis of highly conserved ribosome recycling in eukaryotes and archaea. Nature, 2012, 482, 501-506.	27.8	210
24	Crystal structure of a thermostable type B DNA polymerase from Thermococcus gorgonarius. Proceedings of the National Academy of Sciences of the United States of America, 1999, 96, 3600-3605.	7.1	205
25	Epitope characterization and crystal structure of GA101 provide insights into the molecular basis for type I/II distinction of CD20 antibodies. Blood, 2011, 118, 358-367.	1.4	203
26	Sequence-specific activation of the DNA sensor cGAS by Y-form DNA structures as found in primary HIV-1 cDNA. Nature Immunology, 2015, 16, 1025-1033.	14.5	202
27	Rad50/SMC proteins and ABC transporters: unifying concepts from high-resolution structures. Current Opinion in Structural Biology, 2003, 13, 249-255.	5.7	193
28	Bypass of DNA Lesions Generated During Anticancer Treatment with Cisplatin by DNA Polymerase Î. Science, 2007, 318, 967-970.	12.6	193
29	Structure and Subunit Topology of the INO80 Chromatin Remodeler and Its Nucleosome Complex. Cell, 2013, 154, 1207-1219.	28.9	192
30	Structural basis for ATP-dependent chromatin remodelling by the INO80 complex. Nature, 2018, 556, 386-390.	27.8	188
31	The Mre11:Rad50 Structure Shows an ATP-Dependent Molecular Clamp in DNA Double-Strand Break Repair. Cell, 2011, 145, 54-66.	28.9	182
32	Viral unmasking of cellular 5S rRNA pseudogene transcripts induces RIG-I-mediated immunity. Nature Immunology, 2018, 19, 53-62.	14.5	179
33	Species-specific detection of the antiviral small-molecule compound CMA by STING. EMBO Journal, 2013, 32, 1440-1450.	7.8	162
34	RIG-I detects infection with live <i>Listeria</i> by sensing secreted bacterial nucleic acids. EMBO Journal, 2012, 31, 4153-4164.	7.8	153
35	Structural Biochemistry of ATP-Driven Dimerization and DNA-Stimulated Activation of SMC ATPases. Current Biology, 2004, 14, 1778-1782.	3.9	151
36	Structural basis for sequestration and autoinhibition of cGAS by chromatin. Nature, 2020, 587, 678-682.	27.8	146

#	Article	IF	CITATIONS
37	Structural Framework for the Mechanism of Archaeal Exosomes in RNA Processing. Molecular Cell, 2005, 20, 461-471.	9.7	145
38	GATA2 zinc finger 1 mutations associated with biallelic CEBPA mutations define a unique genetic entity of acute myeloid leukemia. Blood, 2012, 120, 395-403.	1.4	137
39	DNA double-strand break repair from head to tail. Current Opinion in Structural Biology, 2002, 12, 115-122.	5.7	133
40	The ternary microplasmin–staphylokinase–microplasmin complex is a proteinase–cofactor–substrate complex in action. Nature Structural Biology, 1998, 5, 917-923.	9.7	132
41	Rad50-CARD9 interactions link cytosolic DNA sensing to IL-1β production. Nature Immunology, 2014, 15, 538-545.	14.5	132
42	The regulatory domain of the RIG-I family ATPase LGP2 senses double-stranded RNA. Nucleic Acids Research, 2009, 37, 2014-2025.	14.5	131
43	Coagulation factor IXa: the relaxed conformation of Tyr99 blocks substrate binding. Structure, 1999, 7, 989-996.	3.3	123
44	Functional and biochemical dissection of the structure-specific nuclease ARTEMIS. EMBO Journal, 2004, 23, 1987-1997.	7.8	122
45	Mre11 and Rad50 from Pyrococcus furiosus: Cloning and Biochemical Characterization Reveal an Evolutionarily Conserved Multiprotein Machine. Journal of Bacteriology, 2000, 182, 6036-6041.	2.2	116
46	MRE11/RAD50/NBS1: complex activities. Chromosoma, 2004, 113, 157-66.	2.2	113
47	In Vivo Ligands of MDA5 and RIG-I in Measles Virus-Infected Cells. PLoS Pathogens, 2014, 10, e1004081.	4.7	111
48	Point mutations in the juxtamembrane domain of FLT3 define a new class of activating mutations in AML. Blood, 2006, 107, 3700-3707.	1.4	108
49	Dihydrofolate Reductase Deficiency Due to a Homozygous DHFR Mutation Causes Megaloblastic Anemia and Cerebral Folate Deficiency Leading to Severe Neurologic Disease. American Journal of Human Genetics, 2011, 88, 226-231.	6.2	108
50	Structure of Mre11–Nbs1 complex yields insights into ataxia-telangiectasia–like disease mutations and DNA damage signaling. Nature Structural and Molecular Biology, 2012, 19, 693-700.	8.2	108
51	Paramyxovirus V Proteins Disrupt the Fold of the RNA Sensor MDA5 to Inhibit Antiviral Signaling. Science, 2013, 339, 690-693.	12.6	107
52	Common variants in the HLA-DQ region confer susceptibility to idiopathic achalasia. Nature Genetics, 2014, 46, 901-904.	21.4	104
53	Mec1, INO80, and the PAF1 complex cooperate to limit transcription replication conflicts through RNAPII removal during replication stress. Genes and Development, 2016, 30, 337-354.	5.9	103
54	Mechanism of DNA End Sensing and Processing by the Mre11-Rad50 Complex. Molecular Cell, 2019, 76, 382-394.e6.	9.7	100

#	Article	IF	CITATIONS
55	Structural mechanism of <scp>ATP</scp> â€dependent <scp>DNA</scp> binding and <scp>DNA</scp> end bridging by eukaryotic Rad50. EMBO Journal, 2016, 35, 759-772.	7.8	99
56	RG7116, a Therapeutic Antibody That Binds the Inactive HER3 Receptor and Is Optimized for Immune Effector Activation. Cancer Research, 2013, 73, 5183-5194.	0.9	96
57	Human TGF-β1 deficiency causes severe inflammatory bowel disease and encephalopathy. Nature Genetics, 2018, 50, 344-348.	21.4	95
58	ATP driven structural changes of the bacterial Mre11:Rad50 catalytic head complex. Nucleic Acids Research, 2012, 40, 914-927.	14.5	94
59	Snf2 family ATPases and DExx box helicases: differences and unifying concepts from high-resolution crystal structures. Nucleic Acids Research, 2006, 34, 4160-4167.	14.5	93
60	Molecular basis of Rrn3-regulated RNA polymerase I initiation and cell growth. Genes and Development, 2011, 25, 2093-2105.	5.9	87
61	The cytosolic DNA sensor cGAS recognizes neutrophil extracellular traps. Science Signaling, 2021, 14, .	3.6	87
62	The Rad50 Signature Motif: Essential to ATP Binding and Biological Function. Journal of Molecular Biology, 2004, 335, 937-951.	4.2	85
63	Structure and DNA binding activity of the mouse condensin hinge domain highlight common and diverse features of SMC proteins. Nucleic Acids Research, 2010, 38, 3454-3465.	14.5	82
64	The RIGâ€I ATPase domain structure reveals insights into ATPâ€dependent antiviral signalling. EMBO Reports, 2011, 12, 1127-1134.	4.5	81
65	Measuring DNA mechanics on the genome scale. Nature, 2021, 589, 462-467.	27.8	81
66	X-ray Structure of the Complete ABC Enzyme ABCE1 from Pyrococcus abyssi. Journal of Biological Chemistry, 2008, 283, 7962-7971.	3.4	79
67	Crystal Structures of Uninhibited Factor VIIa Link its Cofactor and Substrate-assisted Activation to Specific Interactions. Journal of Molecular Biology, 2002, 322, 591-603.	4.2	75
68	ATP hydrolysis by the viral RNA sensor RIG-I prevents unintentional recognition of self-RNA. ELife, 2015, 4, .	6.0	75
69	Structure and mechanism of the Swi2/Snf2 remodeller Mot1 in complex with its substrate TBP. Nature, 2011, 475, 403-407.	27.8	73
70	Bifunctional PD-1 × αCD3 × αCD33 fusion protein reverses adaptive immune escape in acute myeloid leukemia. Blood, 2018, 132, 2484-2494.	1.4	73
71	xmlns:mml="http://www.w3.org/1998/Math/MathML" display="inline"> <mml:mi>p</mml:mi> qpcollisions at <mml:math xmlns:mml="http://www.w3.org/1998/Math/MathML" display="inline"><mml:msort><mml:mi>s</mml:mi></mml:msort><mml:mo< td=""><td>4.7</td><td>71</td></mml:mo<></mml:math 	4.7	71
72	<pre>display= filline ><finitialiso(t><finitialiso(t><finitialiso(t><finitialiso(t><finitialiso(t><finitialiso(t><finitialiso(t><finitialiso(t><finitialiso(t))) mathvariant="bold">=<finitialiso(t><finitialiso(t><finitialiso(t)) Structural Analysis of Phenothiazine Derivatives as Allosteric Inhibitors of the MALT1 Paracaspase. Angewandte Chemie - International Edition, 2013, 52, 10384-10387.</finitialiso(t)) </finitialiso(t></finitialiso(t></finitialiso(t))) </finitialiso(t></finitialiso(t></finitialiso(t></finitialiso(t></finitialiso(t></finitialiso(t></finitialiso(t></finitialiso(t></pre>	mml:mtext 13.8	:> <mml:mi>Te 70</mml:mi>

#	Article	IF	CITATIONS
73	X-Ray Structure of RLI, an Essential Twin Cassette ABC ATPase Involved in Ribosome Biogenesis and HIV Capsid Assembly. Structure, 2005, 13, 649-659.	3.3	69
74	Converting blood coagulation factor IXa into factor Xa: dramatic increase in amidolytic activity identifies important active site determinants. EMBO Journal, 1997, 16, 6626-6635.	7.8	68
75	Bispecific digoxigenin-binding antibodies for targeted payload delivery. Proceedings of the National Academy of Sciences of the United States of America, 2011, 108, 8194-8199.	7.1	68
76	Discrimination of cytosolic self and non-self RNA by RIG-I-like receptors. Journal of Biological Chemistry, 2017, 292, 9000-9009.	3.4	68
77	Structural biochemistry of nuclear actin-related proteins 4 and 8 reveals their interaction with actin. EMBO Journal, 2011, 30, 2153-2166.	7.8	63
78	Swi2/Snf2 remodelers: hybrid views on hybrid molecular machines. Current Opinion in Structural Biology, 2012, 22, 225-233.	5.7	63
79	The nuclear actin-containing Arp8 module is a linker DNA sensor driving INO80 chromatin remodeling. Nature Structural and Molecular Biology, 2018, 25, 823-832.	8.2	63
80	Invited review: Architectures and mechanisms of ATP binding cassette proteins. Biopolymers, 2016, 105, 492-504.	2.4	62
81	Activating FLT3 Mutants Show Distinct Gain-of-Function Phenotypes In Vitro and a Characteristic Signaling Pathway Profile Associated with Prognosis in Acute Myeloid Leukemia. PLoS ONE, 2014, 9, e89560.	2.5	60
82	RPA Mediates Recruitment of MRX to Forks and Double-Strand Breaks to Hold Sister Chromatids Together. Molecular Cell, 2016, 64, 951-966.	9.7	57
83	Structure of the Rad50 <scp>DNA</scp> doubleâ€strand break repair protein in complex with <scp>DNA</scp> . EMBO Journal, 2014, 33, 2847-2859.	7.8	55
84	Differential Arrangements of Conserved Building Blocks among Homologs of the Rad50/Mre11 DNA Repair Protein Complex. Journal of Molecular Biology, 2004, 339, 937-949.	4.2	53
85	câ€diâ€AMP recognition by <i>Staphylococcus aureus</i> PstA. FEBS Letters, 2015, 589, 45-51.	2.8	52
86	Cathepsin S Alterations Induce a Tumor-Promoting Immune Microenvironment in Follicular Lymphoma. Cell Reports, 2020, 31, 107522.	6.4	50
87	New enzyme lineages by subdomain shuffling. Proceedings of the National Academy of Sciences of the United States of America, 1998, 95, 9813-9818.	7.1	49
88	Mechanisms of nucleic acid translocases: lessons from structural biology and single-molecule biophysics. Current Opinion in Structural Biology, 2007, 17, 87-95.	5.7	48
89	Structure of Actin-related protein 8 and its contribution to nucleosome binding. Nucleic Acids Research, 2012, 40, 11036-11046.	14.5	48
90	Exome sequencing identifies recurring FLT3 N676K mutations in core-binding factor leukemia. Blood, 2013, 122, 1761-1769.	1.4	48

#	Article	IF	CITATIONS
91	Molecular architecture and regulation of BCL10-MALT1 filaments. Nature Communications, 2018, 9, 4041.	12.8	47
92	Structural and functional analysis of Mre11-3. Nucleic Acids Research, 2004, 32, 1886-1893.	14.5	46
93	Dramatic enhancement of the catalytic activity of coagulation factor IXa by alcohols. FEBS Letters, 1997, 412, 295-300.	2.8	45
94	ZBTB7A mutations in acute myeloid leukaemia with t(8;21) translocation. Nature Communications, 2016, 7, 11733.	12.8	45
95	Theory of allosteric effects in serine proteases. Biophysical Journal, 1996, 70, 174-181.	0.5	42
96	Correlating Calcium Binding, Förster Resonance Energy Transfer, andÂConformational Change in the Biosensor TN-XXL. Biophysical Journal, 2012, 102, 2401-2410.	0.5	42
97	Physiological fIXa Activation Involves a Cooperative Conformational Rearrangement of the 99-Loop. Journal of Biological Chemistry, 2003, 278, 4121-4126.	3.4	40
98	The exosome: a macromolecular cage for controlled RNA degradation. Molecular Microbiology, 2006, 61, 1372-1379.	2.5	40
99	Conformational changes of a Swi2/Snf2 ATPase during its mechano-chemical cycle. Nucleic Acids Research, 2008, 36, 1881-1890.	14.5	40
100	MlaA, a hexameric ATPase linked to the Mre11 complex in archaeal genomes. EMBO Reports, 2004, 5, 54-59.	4.5	39
101	Mechanism of replication blocking and bypass of Y-family polymerase by bulky acetylaminofluorene DNA adducts. Proceedings of the National Academy of Sciences of the United States of America, 2010, 107, 20720-20725.	7.1	39
102	Structural Basis for Dodecameric Assembly States and Conformational Plasticity of the Full-Length AAA+ ATPases Rvb1·Rvb2. Structure, 2015, 23, 483-495.	3.3	39
103	Activity-Based Probes for Detection of Active MALT1 Paracaspase in Immune Cells and Lymphomas. Chemistry and Biology, 2015, 22, 129-138.	6.0	36
104	Structural and biochemical characterization of the cell fate determining nucleotidyltransferase fold protein MAB21L1. Scientific Reports, 2016, 6, 27498.	3.3	36
105	Nuclear cGAS: guard or prisoner?. EMBO Journal, 2021, 40, e108293.	7.8	36
106	Sensing of viral nucleic acids by RIG-I: From translocation to translation. European Journal of Cell Biology, 2012, 91, 78-85.	3.6	35
107	Ruler elements in chromatin remodelers set nucleosome array spacing and phasing. Nature Communications, 2021, 12, 3232.	12.8	34
108	The influence of residue 190 in the S1 site of trypsin-like serine proteases on substrate selectivity is universally conserved. FEBS Letters, 2002, 530, 220-224.	2.8	32

#	Article	IF	CITATIONS
109	Impact of Heterogeneity and Lattice Bond Strength on DNA Triangle Crystal Growth. ACS Nano, 2016, 10, 9156-9164.	14.6	31
110	Structural Basis for Transcription-coupled Repair: the N Terminus of Mfd Resembles UvrB with Degenerate ATPase Motifs. Journal of Molecular Biology, 2006, 355, 675-683.	4.2	30
111	Crystal Structure of an Anti-Ang2 CrossFab Demonstrates Complete Structural and Functional Integrity of the Variable Domain. PLoS ONE, 2013, 8, e61953.	2.5	30
112	Genome information processing by the INO80 chromatin remodeler positions nucleosomes. Nature Communications, 2021, 12, 3231.	12.8	27
113	Molecular basis of human ATM kinase inhibition. Nature Structural and Molecular Biology, 2021, 28, 789-798.	8.2	26
114	Unified mechanisms for self-RNA recognition by RIG-I Singleton-Merten syndrome variants. ELife, 2018, 7, .	6.0	26
115	Structure and DNAâ€binding activity of the <i>Pyrococcus furiosus</i> SMC protein hinge domain. Proteins: Structure, Function and Bioinformatics, 2011, 79, 558-568.	2.6	25
116	Structural Studies of DNA End Detection and Resection in Homologous Recombination. Cold Spring Harbor Perspectives in Biology, 2014, 6, a017962-a017962.	5.5	25
117	CD19-specific triplebody SPM-1 engages NK and Î ³ δT cells for rapid and efficient lysis of malignant B-lymphoid cells. Oncotarget, 2016, 7, 83392-83408.	1.8	25
118	Near-Complete Structure and Model of Tel1ATM from Chaetomium thermophilum Reveals a Robust Autoinhibited ATP State. Structure, 2020, 28, 83-95.e5.	3.3	24
119	A modular and controllable T cell therapy platform for acute myeloid leukemia. Leukemia, 2021, 35, 2243-2257.	7.2	24
120	Quantitative analysis of processive RNA degradation by the archaeal RNA exosome. Nucleic Acids Research, 2010, 38, 5166-5176.	14.5	23
121	Mechanistic insight into the assembly of the HerA–NurA helicase–nuclease DNA end resection complex. Nucleic Acids Research, 2017, 45, 12025-12038.	14.5	23
122	Structural and biochemical characterization of human Schlafen 5. Nucleic Acids Research, 2022, 50, 1147-1161.	14.5	23
123	Structural analysis of the diadenylate cyclase reaction of DNA-integrity scanning protein A (DisA) and its inhibition by 3′-dATP. Biochemical Journal, 2015, 469, 367-374.	3.7	22
124	Megadalton chromatin remodelers: common principles for versatile functions. Current Opinion in Structural Biology, 2020, 64, 134-144.	5.7	22
125	Energetics of the thrombin-fibrinogen interaction. Biochemistry, 1992, 31, 11567-11571.	2.5	21
126	Chemical compensation in macromolecular bridge-binding to thrombin. Biochemistry, 1993, 32, 2947-2953.	2.5	21

8

#	Article	IF	CITATIONS
127	Dual-targeting triplebody 33-16-123 (SPM-2) mediates effective redirected lysis of primary blasts from patients with a broad range of AML subtypes in combination with natural killer cells. Oncolmmunology, 2018, 7, e1472195.	4.6	21
128	DNA Mismatch Repair. Structure, 2000, 8, R237-R241.	3.3	20
129	Crystal Structure of Human TWEAK in Complex with the Fab Fragment of a Neutralizing Antibody Reveals Insights into Receptor Binding. PLoS ONE, 2013, 8, e62697.	2.5	19
130	Structure of the catalytic domain of Mre11 from <i>Chaetomium thermophilum</i> . Acta Crystallographica Section F, Structural Biology Communications, 2015, 71, 752-757.	0.8	19
131	The bacterial Mre11–Rad50 homolog SbcCD cleaves opposing strands of DNA by two chemically distinct nuclease reactions. Nucleic Acids Research, 2018, 46, 11303-11314.	14.5	19
132	OAS1/RNase L executes RIG-I ligand–dependent tumor cell apoptosis. Science Immunology, 2021, 6, .	11.9	19
133	Dual-targeting triplebody 33-3-19 mediates selective lysis of biphenotypic CD19+ CD33+ leukemia cells. Oncotarget, 2016, 7, 22579-22589.	1.8	19
134	Structural basis for recognition and remodeling of the TBP:DNA:NC2 complex by Mot1. ELife, 2015, 4, .	6.0	19
135	SIRPα-antibody fusion proteins stimulate phagocytosis and promote elimination of acute myeloid leukemia cells. Oncotarget, 2017, 8, 11284-11301.	1.8	17
136	Lessons from structural and biochemical studies on the archaeal exosome. Biochemical Society Transactions, 2009, 37, 83-87.	3.4	16
137	ATP puts the brake on DNA doubleâ€strand break repair. BioEssays, 2014, 36, 1170-1178.	2.5	16
138	A Click hemistry Linked 2′3′ GAMP Analogue. Chemistry - A European Journal, 2019, 25, 2089-2095.	3.3	16
139	Molecular architecture of the HerA–NurA DNA doubleâ€strand break resection complex. FEBS Letters, 2014, 588, 4637-4644.	2.8	15
140	DNA Double-Strand Breaks Come into Focus. Cell, 2009, 139, 25-27.	28.9	14
141	Rustless translation. Biological Chemistry, 2012, 393, 1079-1088.	2.5	13
142	SIRPα-αCD123 fusion antibodies targeting CD123 in conjunction with CD47 blockade enhance the clearance of AML-initiating cells. Journal of Hematology and Oncology, 2021, 14, 155.	17.0	13
143	Reversible and Controllable Nanolocomotion of an RNA-Processing Machinery. Nano Letters, 2010, 10, 5123-5130.	9.1	12
144	NK cells from an AML patient have recovered in remission and reached comparable cytolytic activity to that of a healthy monozygotic twin mediated by the single-chain triplebody SPM-2. Journal of Translational Medicine, 2013, 11, 289.	4.4	12

#	Article	IF	CITATIONS
145	Response to: Monoclonal antibodies targeting CD20. MAbs, 2013, 5, 337-338.	5.2	12
146	Singleâ€nolecule nucleosome remodeling by <scp>INO</scp> 80 and effects of histone tails. FEBS Letters, 2018, 592, 318-331.	2.8	12
147	Biochemical Characterization and Crystal Structure of a Dim1 Family Associated Protein:  Dim2. Biochemistry, 2005, 44, 11997-12008.	2.5	11
148	BusR senses bipartite DNA binding motifs by a unique molecular ruler architecture. Nucleic Acids Research, 2021, 49, 10166-10177.	14.5	11
149	Structural Basis for Adenylate Kinase Activity in ABC ATPases. Journal of Molecular Biology, 2010, 401, 265-273.	4.2	10
150	Chromosome Biology: The Crux of the Ring. Current Biology, 2006, 16, R102-R105.	3.9	8
151	Structure–Function Analysis of SWI2/SNF2 Enzymes. Methods in Enzymology, 2006, 409, 375-388.	1.0	8
152	Serendipitous crystallization and structure determination of cyanase (CynS) from <i>Serratia proteamaculans</i> . Acta Crystallographica Section F, Structural Biology Communications, 2015, 71, 471-476.	0.8	8
153	DuoMab: a novel CrossMab-based IgG-derived antibody format for enhanced antibody-dependent cell-mediated cytotoxicity. MAbs, 2019, 11, 1402-1414.	5.2	8
154	Structural basis of the (in)activity of the apical DNA damage response kinases ATM, ATR and DNA-PKcs. Progress in Biophysics and Molecular Biology, 2021, 163, 120-129.	2.9	8
155	Nuclear actin-related proteins take shape. Bioarchitecture, 2011, 1, 192-195.	1.5	7
156	RIG-I Holds the CARDs in a Game of Self versus Nonself. Molecular Cell, 2014, 55, 505-507.	9.7	7
157	Chip-based platform for dynamic analysis of NK cell cytolysis mediated by a triplebody. Analyst, The, 2016, 141, 2284-2295.	3.5	7
158	Chemical Synthesis of the Fluorescent, Cyclic Dinucleotides c th GAMP. ChemBioChem, 2022, 23, .	2.6	7
159	Binding of Fibrinogen Aα1–50-β-Galactosidase Fusion Protein to Thrombin Stabilizes the Slow Form. Journal of Biological Chemistry, 1995, 270, 24790-24793.	3.4	6
160	Processive RNA decay by the exosome. RNA Biology, 2011, 8, 55-60.	3.1	6
161	Envisioning the Fourth Dimension of the Genetic Code: The Structural Biology of Macromolecular Recognition and Conformational Switching in DNA Repair. Cold Spring Harbor Symposia on Quantitative Biology, 2000, 65, 113-126.	1.1	6
162	T cell-recruiting triplebody 19-3-19 mediates serial lysis of malignant B-lymphoid cells by a single T cell. Oncotarget, 2014, 5, 6466-6483.	1.8	6

#	Article	IF	CITATIONS
163	Symmetry conditions for binding processes Proceedings of the National Academy of Sciences of the United States of America, 1992, 89, 2727-2731.	7.1	5
164	Crystal and solution structure of the human RIG-I SF2 domain. Acta Crystallographica Section F, Structural Biology Communications, 2014, 70, 1027-1031.	0.8	4
165	RIG-I-Like Receptors: One STrEP Forward. Trends in Microbiology, 2016, 24, 517-519.	7.7	4
166	Crystal structure of the full Swi2/Snf2 remodeler Mot1 in the resting state. ELife, 2018, 7, .	6.0	4
167	Evaluation of a Bifunctional Sirpα-CD123 Fusion Antibody for the Elimination of Acute Myeloid Leukemia Stem Cells. Blood, 2019, 134, 2544-2544.	1.4	3
168	Chromosome Cohesion: Closing Time. Current Biology, 2003, 13, R866-R868.	3.9	1
169	The exosome, plugged. EMBO Reports, 2007, 8, 456-457.	4.5	1
170	Crystallization of Mouse RIG-I ATPase Domain: In Situ Proteolysis. Methods in Molecular Biology, 2014, 1169, 27-35.	0.9	1
171	Exploiting an Anti-CD3/CD33 Bispecific Antibody to Redirect Donor T Cells Against HLA Loss Leukemia Relapses. Blood, 2019, 134, 513-513.	1.4	1
172	The chemistry of transcription through damaged DNA and of translesion synthesis at atomic resolution. Nucleic Acids Symposium Series, 2007, 51, 103-103.	0.3	0
173	Structure and Function of Rad50/SMC Protein Complexes in Chromosome Biology. , 2005, , 201-218.		Ο
174	Single Molecule Study Of the RNA Degradation and Polyadenylation Activities of the Archaeal Exosome. Biophysical Journal, 2009, 96, 367a.	0.5	0
175	232 Unique molecular recognition of CD20 by the type II CD20 antibody GA101. European Journal of Cancer, Supplement, 2010, 8, 75-76.	2.2	0
176	Strukturelle Analyse von Phenothiazinâ€Đerivaten als allosterische Inhibitoren der MALT1â€Paracaspase. Angewandte Chemie, 2013, 125, 10575-10579.	2.0	0
177	Editorial overview: Theory and simulation: Macromolecular machines. Current Opinion in Structural Biology, 2014, 25, vi-viii.	5.7	0
178	Single-Molecule Choreography between Telomere Proteins and G Quadruplexes. Structure, 2014, 22, 801-802.	3.3	0
179	Catalytic Mechanism of the INO80 Chromatin Remodeler Acting on the Nucleosome. Biophysical Journal, 2016, 110, 236a.	0.5	0
180	Editorial overview: Macromolecular machines and assemblies. Current Opinion in Structural Biology, 2016, 37, vi-viii.	5.7	0

#	Article	IF	CITATIONS
181	Dissecting the Mechanism of the HerA NurA DNA Break Resection Complex using Native Mass Spectrometry. Biophysical Journal, 2017, 112, 515a.	0.5	0
182	Mechanistic Insight into the Assembly of the HerA-NurA Helicase-Nuclease DNA End Resection Complex using Native Mass Spectrometry. Biophysical Journal, 2018, 114, 440a.	0.5	0
183	The Mre11/Rad50/Nbs1 Complex. , 2005, , .		0
184	Point Mutations Found in the Juxtamembrane Domain of FLT3 Define a New Class of Activating Mutations in AML Blood, 2005, 106, 4388-4388.	1.4	0
185	Chapter 5. RIG-I-Like RNA Helicases: Multidomain Proteins in Antiviral Innate Immunity and Processing of Small Regulatory RNAs. RSC Biomolecular Sciences, 2010, , 121-148.	0.4	0
186	Insights into DNA damage signaling from the structure of an Mre11:Nbs1 complex. FASEB Journal, 2010, 24, lb39.	0.5	0
187	The RNA Exosomes. Nucleic Acids and Molecular Biology, 2011, , 223-244.	0.2	0
188	Aberrant Cathepsin S Induces a Supportive Immune Microenvironment in Follicular Lymphoma. Blood, 2019, 134, 657-657.	1.4	0